

2 PHIL photoinjector test line*

M. Alves^a, C. Arnault^a, D. Auguste^a, J.L. Babigeon^a, F. Blot^a, J. Brossard^a, C. Bruni[†], S. Cavalier^a, J.N. Cayla^a, V. Chaumat^a, J. Collin^a, M. Dehamme^a, M. Demarest^a, J.P. Dugal^a, M. Elkhaldi^a, I. Falleau^a, A. Gonnin^a, M. Jore^a, E. Jules^a, B. Leluan^a, P. Lepercq^a, F. Letellier^a, E. Mandag^a, J.C. Marrucho^a, B. Mercier^a, E. Mistretta^a, C. Prevost^a, R. Roux^a, V. Soskov^a, A. Toutain^a, A. Variola^a, O Vitez^a, H. Monard^{a‡}

^a*Laboratoire de l'accélérateur linéaire,*

Université Paris-Sud 11, UMR 8607, Bâtiment 200, 91898 Orsay Cedex, France

3 *E-mail: bruni@lal.in2p3.fr*

ABSTRACT: LAL is now equipped with its own platform for photoinjectors tests and Research and Development, named PHIL (PHotoInjectors at LAL). This facility has two main purposes: push the limits of the photoinjectors performances working on both the design and the associated technology and provide a low energy (MeV) short pulses (ps) electron beam for the interested users. Another very important goal of this machine will be to provide an opportunity to form accelerator physics students, working in a high technology environment To achieve this goal a test line was realised equipped with an RF source, magnets and beam diagnostics. In this article we will describe the PHIL beamline and its characteristics together with the description of the first two photoinjector realised in LAL and tested: the ALPHAX and the PHIN RF Guns.

5 **KEYWORDS:** photoinjector, electron source.

*Web site of the project :<http://phil.lal.in2p3.fr/>

[†]Corresponding author: bruni@lal.in2p3.fr

[‡]Project manager: monard@lal.in2p3.fr

7 Contents

8	1. Introduction	1
9	2. PHIL RF guns and their sub-systems	2
10	2.1 PHIN gun	3
11	2.2 AlphaX	4
12	2.3 RF power source	4
13	2.4 Laser	5
14	2.5 Timing	6
15	2.6 Vacuum	7
16	2.7 Control systems	8
17	2.8 RF commissioning of the guns	9
18	3. Magnetic elements	10
19	4. Diagnostics	11
20	4.1 Electron beam energy and its dispersion	11
21	4.2 Charge	11
22	4.3 Transverse dimensions	12
23	4.4 Bunch length	14
24	4.5 Transverse emittance	15
25	5. Conclusion	15
26	6. Acknowledgments	15

28 1. Introduction

29 For many years LAL (Laboratoire de L'Accélérateur Linéaire at Orsay, France) has built RF guns
 30 for different projects starting with CANDELA [1] at Orsay, France going to ALPHAX for Stratch-
 31 lyde university [2] in the UK, ELYSE [3] for the Laboratoire de Chimie-Physique at Orsay and
 32 recently for the probe beam and the test beam at CERN/CTF3 [4, 5, 6]. At present LAL is equipped
 33 with its own photoinjector test line named PHIL (PHotoInjector at LAL) proposed in the European
 34 Community REsearch Infrastructure Activity CARE [7] ¹ able to work with several RF guns at 3
 35 GHz.

36 PHIL was designed for two main purposes :

¹We acknowledge the support of the European Community-Research Infrastructure Activity under the FP6 "Structuring the European Research Area" programme (CARE, contract number RII3-CT-2003-506395), <http://www.infn.it/phin>

- 37 • research and development on the electron sources,
- 38 • providing the beam to users interested in a low energy (9 MeV), low emittance short pulse
- 39 (5 ps) electron beam.

40 The research and development program for PHIL is driven by the will to obtain high gradient
 41 electric field up to 100 MV/m, subpicosecond electron beam duration, photocathodes with longer
 42 lifetime, a lower dark current, a better understanding of the electron beam dynamics inside the
 43 gun, the comparison between different RF guns and cathodes, and pushing the limits of the number
 44 of cells for an RF gun [8], etc... PHIL will also be a platform for welcoming users interested
 45 in a low emittance, well defined energy, low energy electron beam. For example measuring the
 46 fluorescence of air in high atmosphere conditions will help to improve the precision of the measure
 47 of the primary particle energy of cosmic rays[9]. Another purpose sought by PHIL is the training of
 48 the engineers, technicians and students that the accelerator community will need in the near future
 49 for other accelerator projects involving photoinjectors, like THOMX [10] for example.

50 PHIL is a photoinjector beamline (see fig. 1), whose configuration evolves in time. Today
 51 PHIL is equipped with a copper photocathode RF gun, vacuum chambers with ionic pumps and
 52 magnetic elements: 2 coils on the RF gun, 2 steerers to correct the orbit, a coil in the middle of the
 53 beamline and a dipole used as a spectrometer to measure the energy of the beam. The transverse
 54 positions of the electron beam are measured with Beam Position Monitors (BPM). The charge is
 55 measured with Faraday cups at both ends of the beamline and also with two Integrating Current
 56 Transformers (ICT from the Berghoz company). This setup is allowing us to measure the transport
 57 line charge transmission. The transverse sizes of the electron beam are measured with the light
 58 emitted by YAG:Ce screen stations coupled to CCD cameras [11].

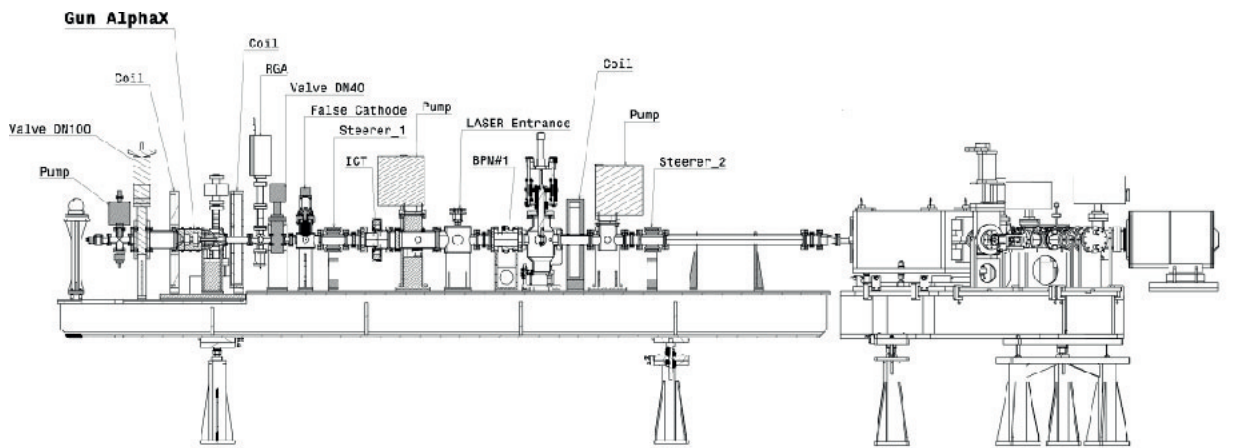


Figure 1. Mechanical drawing of PHIL test line

59 This article will describe the PHIL photoinjector beam line which is made up of 3 GHz RF
 60 gun, a laser system, and a beam line diagnostics.

61 2. PHIL RF guns and their sub-systems

62 At the beginning of the project PHIL, in 2004, the goal was to test the PHIN RF guns that LAL

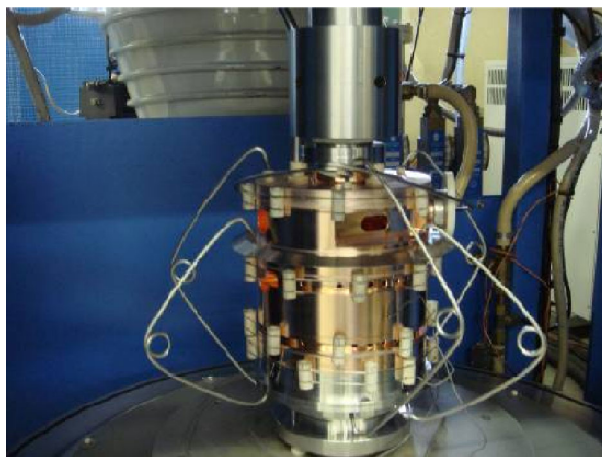


Figure 2. picture of cells of the PHIN gun before their brazing under vacuum. The wires and the small ceramic tubes ensure that the cells are well centered. The load at the top and the springs guarantee the contact between surfaces which will be brazed.

63 was manufacturing for CERN. It was carried out as part of a work package of a joint research
 64 activity in the network CARE of the 6th Framework Program of the European Union. In addition
 65 to the construction of a photo-injector for CERN, LAL build its own beamline to do research and
 66 development on photoinjector technology.

67 These two RF guns have been totally built by the mechanical department of LAL. The design
 68 was performed jointly with the CERN experts and the workshop achieved the precise tolerances that
 69 are needed to fulfill both the RF and the brazing under vacuum constraints. A big effort was also
 70 produced to understand and optimise the different thermal cycles. This was needed to guarantee a
 71 successful brazing under vacuum. In picture 2, you can see the PHIN gun, foreseen to be installed
 72 at PHIL, before one of the five brazing steps.

73 The alphaX-RF gun was installed to start with and this allowed us to get a first electron beam
 74 at the end of 2009. The characterization of the beam produced is still ongoing. The drawback
 75 of the alphas RF gun is that, its cathode cannot be changed without a vacuum intervention. The
 76 next RF gun to be mounted on PHIL, will be the PHIN RF gun which has the advantage of quick
 77 cathode changing without any vacuum breaking. Behind the RF gun will be placed a cathode holder
 78 coupled itself to four cathode chamber receiver. This last chamber can be coupled on the CERN
 79 preparation cathode laboratory, so that different cathodes can be evaporated, transferred to Orsay,
 80 and tested on PHIL.

81 **2.1 PHIN gun**

82 This photoinjector was designed to be the source of electrons for the drive beam linac of the CLIC
 83 Test Facility 3 (CTF3) at CERN [12]. The specifications of CERN for this gun were rather demand-
 84 ing: produce around 2300 bunches of 2.33 nC each during the RF pulse of $2.5 \mu\text{s}$ with emittance
 85 below $20 \pi\text{mmrad}$ and energy spread below 2 %. It was decided that the design should rely on
 86 the long past experience of CERN in producing a high charge electron beam with photo-injector
 87 [4]. The photo-injector has 2.6 cells at 2.998 GHz of resonant frequency, a schematic is shown
 88 in figure 3. The diameter of inner irises is rather large, 40 mm, to accommodate the high charge.

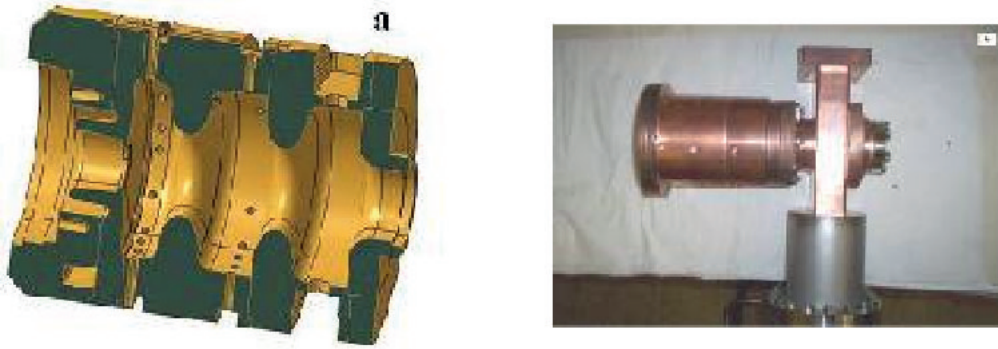


Figure 3. a) PHIN gun, b) AlphaX gun

89 The RF features are summarized in table 1. Irises were machined with an elliptical shape which
 90 reduces the surface electrical field by 20 % with respect to a cylindrical shape according to the RF
 91 simulations [5, 13]. In addition waveguides are symmetrically connected to the last cavity of the
 92 gun with respect to the mechanical axis in order to reduce emittance degradation induced by a non
 93 isotropic electrical field. The dimensions of the coupling apertures have been calculated in order
 94 to be at the critical coupling taking into account the strong beam loading induced by the electron
 95 beam, which average current in the drive beam linac is 3.5A Without beam, the coupling is roughly
 96 3, divided into equal parts on both input waveguides. On this last point the operation will be dras-
 97 tically different on PHIL. Indeed for reasons of cost the laser of PHIL can deliver a single pulse at
 98 a repetition rate ranging from 5 to 100Hz. Therefore there will be no beamloading which means
 99 that the PHIN gun, on PHIL, will stay overcoupled. In order to decrease the reflection factor we
 100 decided to close one input port with a short circuit which allows us to keep the symmetry of the
 101 electrical field in the gun while reducing the reflected power by a factor 4.

102 2.2 AlphaX

103 This gun has been installed on PHIL since 2009 and the first electron beam measurements were
 104 made with it. It is a copy of the photo-injector built by LAL for the ALPHAX accelerator in
 105 the University of Strathclyde in the UK [2]. The design of this gun was done by the Eindhoven
 106 University of Technology. It is also made of 2.5 cells at 2.998 GHz in the π mode, a picture is
 107 shown in figure 3 and also has elliptical irises. However the aperture of the irises is smaller than
 108 in the PHIN gun, 24 mm instead of 40 mm because the requirement of the extracted charge for
 109 AlphaX was 100 pC. But the main difference with respect to the PHIN gun is the coupling between
 110 the gun and waveguides which is done by a co-axial "doorknob" antenna in the cut-off tube after the
 111 cells of the gun. In this way the gun keeps a perfect cylindrical symmetry in order to avoid possible
 112 degradation of the emittance rising in non-symmetric coupling. RF characteristics are summarized
 113 in table 1.

114 2.3 RF power source

115 The RF power needed for the gun is produced by a 25MW klystron (Thomson F2040E). LAL has
 116 built a classical Pulse Forming Network modulator for the biasing of this klystron. This modulator

	PHIN	AlphaX
R_s (M Ω /m)	34	34
Q	14530	11010
β	1.5	1

Table 1. RF characteristics of the RF guns used in PHIL; R_s is the shunt impedance, Q the quality factor and β the coupling factor.

117 is made of an industrial high voltage supply (Technix SR20 20kV-0.4A) charging a Pulse Form
 118 Network (PFN) of 12 cells allowing a pulse length of 5 μ s. The PFN is switched to a high voltage
 119 transformer (Stangeness) using a thyatron (E2V 1525AWX). This system is able to deliver pulses
 120 of 240kV/5 μ s/5Hz at the cathode of the klystron. A low power RF signal (350W/3 μ s, Nuclitudes
 121 pre-amplifier) drives the klystron, the amplitude of the output RF power is modulated by variation
 122 of this low level signal. The klystron is protected from power reflection by a four port phase shift
 123 circulator. A standard WR284 waveguide network propagates the power to the gun. The RF power
 124 is monitored at the output of the klystron and at the gun using two bi-directional couplers and
 125 crystal detectors. The wave guide network is under a 2 bars pressure of SF6, and RF windows
 126 isolate the klystron and the RF gun from the SF6.

127 Power couplers at the exit of the klystron, and just before the RF gun allows a measurement
 128 of the different signals (see fig. 4), as the power going out of the klystron (P_{ik}), the reflected power
 129 to the klystron (P_{rk}), the power going inside the RF gun (P_{ic}) and the reflected power from the
 130 RF gun (P_{rc}). Measurement of the pulse to pulse stability at 5 Hz have shown that it is better than
 131 $2 \cdot 10^{-3}$

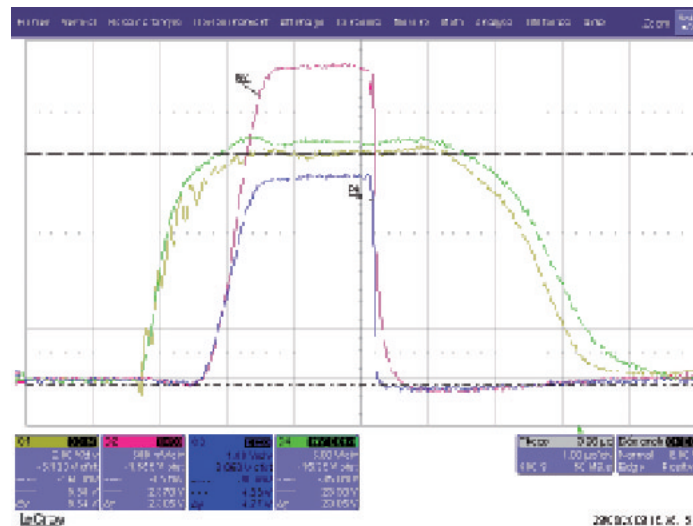


Figure 4. Measurement of I_k klystron intensity (yellow), U_k klystron voltage (green), P_{ik} output power of the klystron (blue), P_{rk} reflected power at the klystron (pink). The klystron was delivering 13MW

132 2.4 Laser

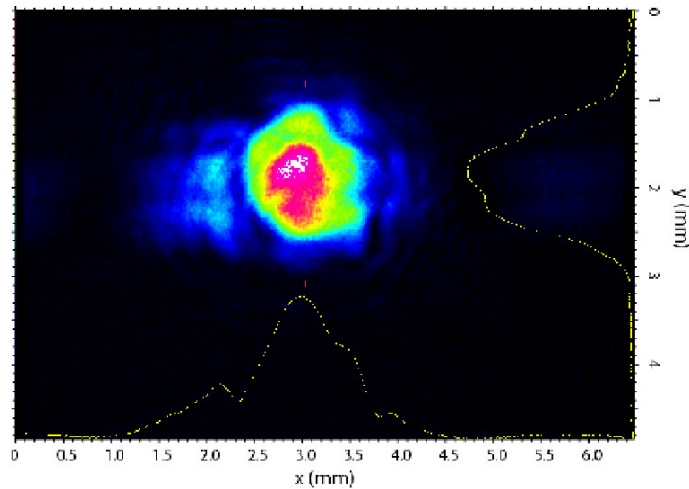
133 A Nd:YLF picosecond mode locked laser, model IC-262-40ps from ‘High Q Laser’ company, is

134 used to illuminate the photocathode. It consists of a SESAM passively mode locked picosecond
135 oscillator, a regenerative amplifier and two frequencies converters and provides $80\mu J \pm 0.3\mu J$
136 pulse energy ($\lambda = 266nm$) at 9ps pulses with a pulse repetition frequency up to 100Hz.

137 The laser oscillator can be locked to the external reference clock (frequency 75MHz) coming
138 from the pilot with the trigger better than 1ps (RMS). The laser pulse to pulse energy stability
139 is near 1% for roughly 8 hours. The output beam is shaped with the help of the iris aperture, and
140 collimated by convex lens (2m-focal). After going through the optical transport line (15m enclosed
141 within a black plastic tube) the beam is focalized on the cathode by the 2m-focal lens at nearly
142 normal incidence on the photocathode plane. The diameter of the laser spot on the photocathode is
143 zoomed by means of the shifting of focusing lens and variation of the iris diameter. The spot size
144 is controlled through an image of the cathode position and has a diameter about 1mm (see fig. 5).
145 The beam point stability (standard deviation) on the cathode is $40\mu m$.

146 A streak camera (ARP) is used to check the pulse duration by sending the 266 nm attenuated
147 light directly to the camera.

148 In the future, developments on the laser will include, obtaining a flat top transverse energy
149 distribution, a simple telescope system to vary the beam diameter continuously, and a stabilization
150 system of the laser transverse position. The image of the laser will be captured with a dedicated
151 UV camera. A feedback system will be installed based on the monitoring of the beam centroid
position with a 4-quadrants diode to move accordingly the mirrors with micrometric translators.



152 **Figure 5.** Image taken with a UV CCD camera. The laser spot is observed on the virtual cathode on the 4th
harmonic of the laser at 262 nm

153 2.5 Timing

154 Three main frequencies are used : 3 GHz for the RF wave, 5 Hz for the election bunch production
155 and 75 MHz for the synchronisation signal. All the signals used on the accelerator are synchronised
156 with a master-clock provided by the RF pilot (see fig. 6).

157 This master clock has a frequency of 75MHz and is created by an Oven Control Crystal Os-
158 cillator (OCCO), whose stability is 10^{-7} . A PLL (Phase Locked Loop) is locked on the master

159 clock to create the low level RF signal (LLRF) at the frequency of 2998.55 MHz, used for the
 160 accelerating structures. The phase of the LLRF is controlled by two adjustable phase-shifters.

161 The timing electronic system delivers all the slow signals synchronised on the master clock.
 162 Several PCI6602 National Instruments cards create the different TTL timing signals which trigger
 163 all the elements of the accelerator (RF pulse, laser pulse, diagnostics). For example, one timing
 164 signal triggers an RF switch to modulate the LLRF and so create the RF pulse that will drive the
 165 power source. Another one monitors the laser pulse at 75 MHz. All these signals have a repetition
 166 rate of 5Hz, their duration can be selected by the users from the command control computer.

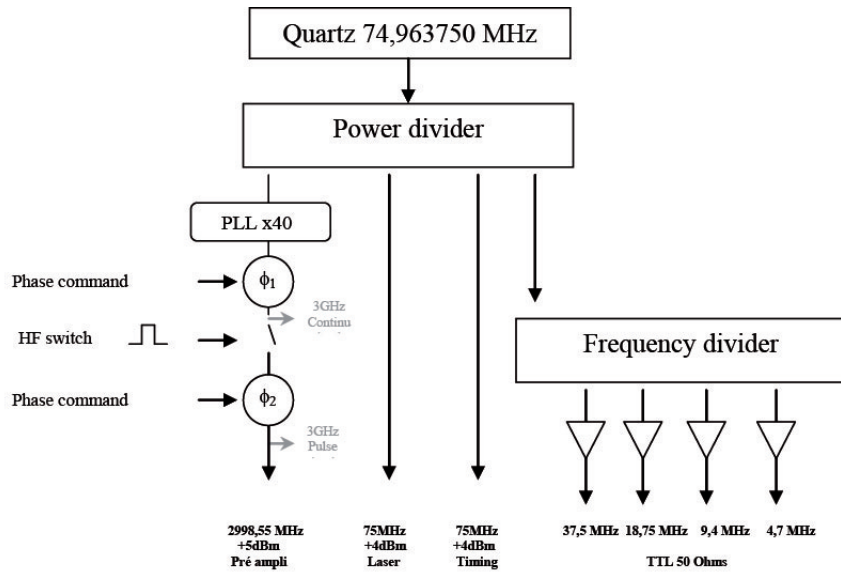


Figure 6. Principle of the RF pilot

167 **2.6 Vacuum**

168 One of the aims of PHIL is to use and test different photocathodes. Although, some alkaline
 169 photocathodes needs an ultra high vacuum (i.e. few 10^{-10} mbar) to increase its lifetime. Then,
 170 the pumping distribution was calculated (see fig. 7) to take into account that the downstream
 171 outgassing sources disturb the pressure minimally in the first half cell of the gun. For that purpose,
 172 ionic pumps (IP) were installed on the waveguides (2 IP starcell at 65L/s) and at the gun exit (1 IP
 173 starcell at 34L/s). A particular precaution was brought to the materials choices and to their thermal
 174 treatments. The PHIL components underwent UHV cleaning and vacuum baking of 450° C at
 175 10^{-6} mbar for five days. At present, the pressure obtained at the level of the copper cathode of the
 176 alphaX gun is satisfactory in $2 \cdot 10^{-9}$ mbar without in situ baking. The dynamic pressure remains
 177 suitable and increases by a factor 4 for a gun working at the temperature of 41° C. By cons, for
 178 the PHIN gun, which will receive alkaline photocathode, NEG coating was done on the gun output
 179 chamber to further improve the vacuum level. This will allow us to reach the $2 \cdot 10^{-10}$ mbar level.
 180 Along the test line, ionic pumps were installed on the transport line (2 IP starcell at 125L/s) and
 181 upstream to every beam dump (1 IP starcell at 50L /s).

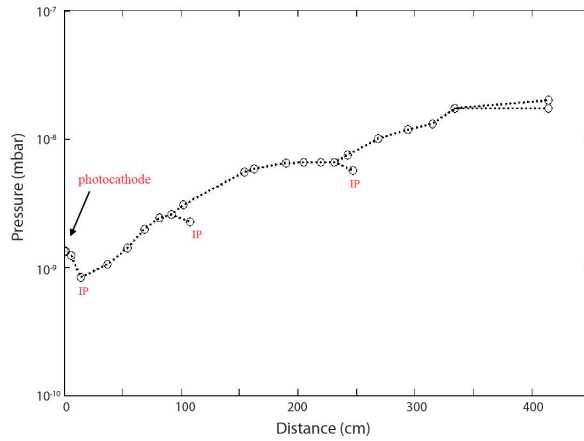


Figure 7. Pressure distribution without in situ baking. Outgassing rate $\tau=5 \cdot 10^{-11}$ mbar l s⁻¹ cm⁻² (eq. N₂)

182 **2.7 Control systems**

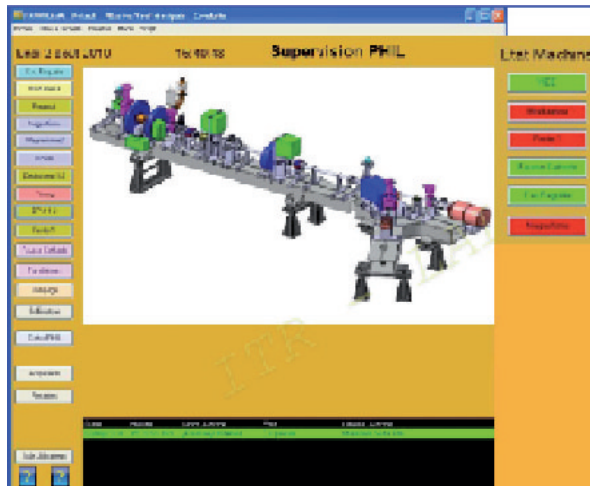


Figure 8. The homepage of PHIL supervision (with Panorama software)

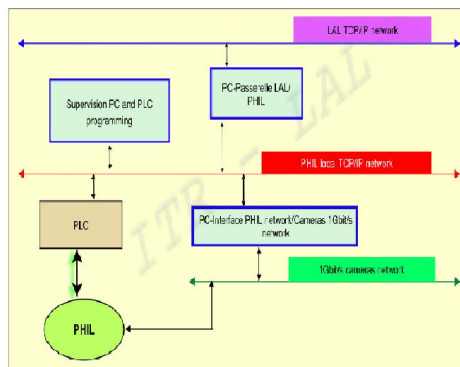


Figure 9. Architecture of the PHIL control command

183 PHIL Command Control is centered on the monitoring soft ware PANORAMATM (see fig.
 184 8) of the company CODRA under Windows XP and Ethernet private network, dedicated to the
 185 Command Control of PHIL. The Architecture is illustrated in figure 9. The interface between the
 186 supervision and control actuators and / or control is performed by PLCs (Wago) and industrial PCs.
 187 The communication protocol is the Modbus that through OPC servers can exchange the orders of
 188 Control and read or write variables to Control. Supervision also allows connection to an MSSQL
 189 database (Microsoft) to store recoverable acquisitions from the laboratory network. This allows a
 190 web application to have a representation of the vacuum state for example (only from the laboratory
 191 network) or the state of the machine (accessible from the global network).

192 2.8 RF commissioning of the guns

193 Nowadays, the two guns have been conditioned : AlphaX up to 92MV/m and partially PHIN to
 194 40MV/m.

195 For five days (around 40h RF), the AlphaX RF commissioning was achieved in two phases
 196 : at first the conditioning was done just to be able to produce a first low energy beam, with
 197 an input power of 4 MW inside the gun, in November 2009. Then the gradient inside the gun
 198 was increased on the beginning of 2010, and the gradient limit was tested. The incident power
 199 from the klystron was increased slowly, the vacuum and reflected power (see fig. 10a) of the gun
 200 were monitored. Some breakdowns occurred, but without damage, the vacuum level in the gun
 201 remained below $5 \cdot 10^{-8}$ mbar during most of the process (see fig. 10b). Finally the klystron reached
 202 11MW, corresponding to 10MW in the gun. Taking into account the RF losses and the coupling
 203 we succeeded in injecting 10 MW in the alphaX RF gun, which corresponds to an accelerating
 204 gradient of 92 MV/m. To reach higher values, we have taken into account an adiabatic approach
 205 in the conditioning procedure (time consuming). During the conditioning of the gun the vacuum
 206 composition was analysed with an RGA quadrupole placed as close as possible to the gun exit. It
 207 showed that gases emitted inside the gun are mostly CO₂ and H₂O.

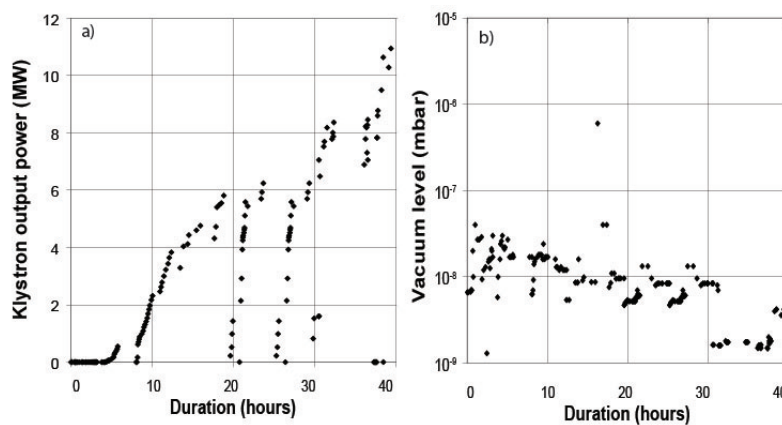


Figure 10. a) Klystron output power versus time and b) gun vacuum level versus time during conditioning of the photoinjector AlphaX

208 3. Magnetic elements

209 In order to optimize beam quality and transport of the beam along the line, magnetic elements were
210 installed. PHIL beamline consists of the three solenoids, two around the RF Gun, one at 2.266m
211 from the cathode plane, two steerers and one dipole.

212 The two solenoids around the gun are a bucking coil and a focusing coil. The former cancels
213 the magnetic field in the photo-cathode plane and the other is used to focus the particles at the exit of
214 the gun. The positions of the coils have been calculated and optimized to limit the emittance growth
215 due to space charge forces. The magnetic field calculated to keep this low emittance value is 0.25T
216 at 2nC and $E_{acc}=85\text{MV/m}$. The design of the coils was optimized for the PHIN gun geometry. It
217 involved constraints on the dimensions of the coil. First, along the longitudinal axis, the minimum
218 distance between the bunching coil and the focusing one could only be 11cm. Secondly, due to
219 the presence of a vacuum chamber around the RF gun, the inner diameter of the coils is rather
220 large. It is then necessary to optimize the number of windings, the diameters and the current in
221 order to stay within the limits imposed by the material while fulfilling the specification to reach
222 a maximum magnetic field of 0.28T. The solenoid were manufactured by a private company SEF.
223 The conductor used for windings is a square copper cable, $6\times 6\text{ mm}^2$ with a hollow in the center of
224 4mm diameter for water cooling. The focusing coil has 208 windings and the other one 100. The
225 Brucker power supply can produce a maximal current of 400A allowing one to reach the magnetic
226 field of 0.28T.

227 However let's note that up to now, it is the ALPHAX RF gun that was installed on PHIL. As
228 this rf gun has a different geometry, the magnetic configuration is different as, for example, the
229 distance between coils. The cancelation of the solenoidal field at the cathode plane [14] is possible
230 with this gun but with a different set up than PHIN gun. The last solenoid located in the middle of
231 the beam line is also used to focus particles, like a quadrupole triplet would have done. But looking
232 at the energy range and the cost, a solenoid fulfills all the requirements needed. This solenoid
233 is able to reach a maximum magnetic field of 0.5T. It has an inner diameter of 70mm and 208
234 windings. The measured calibration of the three solenoids is illustrated in figure 11. The emittance
235 compensation coil exhibits a non linearity [15], which implies variation of its magnetic length with
236 the magnetic field amplitude.

237 The two steerers are used to correct the orbit. One is located roughly 70cm after the output of
238 the gun and one just before the dipole. Technically, they consists of 40 turns in each coil allowing a
239 maximum magnetic field of 20G for an intensity of 5A. The power supply of this magnet is bipolar
240 going from -5A to 5A to allow bending in opposite directions. With these steerers, the trajectory
241 can be changed up to 10mrad.

242 Concerning the dipole, it was made originally for TTF injector [16] and was used with a
243 maximum magnetic field of 0.1T for 20A. This dipole is now used as a spectrometer to measure
244 the beam energy. This is a C-dipole (with face angle of 18.24°) with a curvature radius of 0.7m and
245 a bending angle of 60° . Magnetic measurements were done at CERN to map the magnetic field.
246 This dipole reaches a magnetic field of 421.5G for 8.6A corresponding to the maximum energy of
247 10MeV.

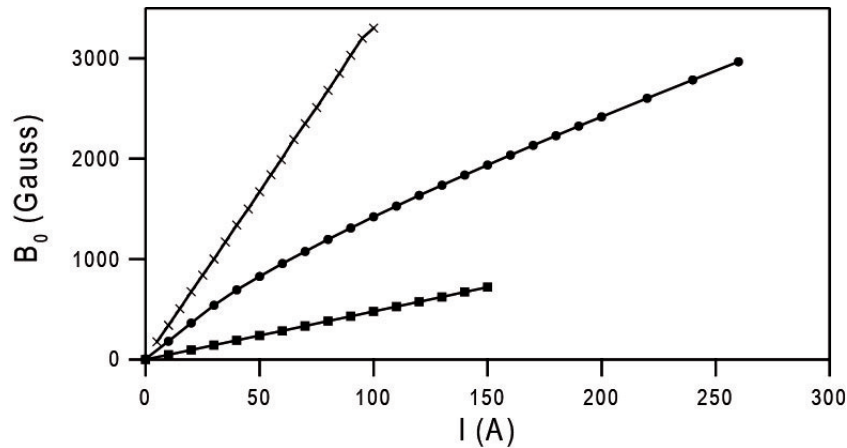


Figure 11. Measurement of the maximum on axis magnetic field versus current for the three solenoids of PHIL line: circle) emittance compensation coil at the exit of the gun, square) bucking coil and cross) focusing coil. The emittance compensation coil exhibits a non linearity resulting in a variation of its magnetic length depending on the current.

248 4. Diagnostics

249 4.1 Electron beam energy and its dispersion

250 On the PHIL Beamline, the dipole is used as a spectrometer to measure the energy of the beam.
 251 Placed after the dipole a collimator is used to analyse the energy distribution. The collimator is
 252 made of 2 copper blocks actuated separately at 90° from the beam axis. This produces a slit with
 253 an adjustable size (from 1mm to 50mm) and position (± 25 mm from the beam axis). A stepper
 254 motor and a precise angular encoder were used to achieve the required accuracy (± 0.1 mm in slit
 255 dimensions and ± 0.1 mm in position) (see picture 13). Measurements and load tests were per-
 256 formed before the fabrication of the device. This collimator was fabricated in the LAL workshops.

257 The electron beam energy dispersion is directly related to the size of the beam by the dispersion
 258 function, in the focal plane of the dipole. Measuring the beam size leads to measurement of the
 259 energy dispersion as a YAG:Ce screen is placed close to the dipole focal plane. An example is
 260 shown in figure 12.

261 4.2 Charge

262 The charge is measured (see fig. 14) with Faraday cups at both ends of the beamline and also with
 263 two Integrating Current Transformer installed in front of the Faraday cup at the end of the straight
 264 beam line and one just after the gun.

265 The extracted charge is a key parameter to control for some applications like detector calibra-
 266 tion for example. It is measured simultaneously with a Faraday cup and an ICT (less than 10 pC to
 267 2nC) at the end of the beam line, these two devices have been calibrated and are in good agreement.
 268 First experiments give an extracting charge of 500 pC (± 10 pC) with a laser pulse energy of 50
 269 μ J (with a fluctuation of 0.5 μ J).

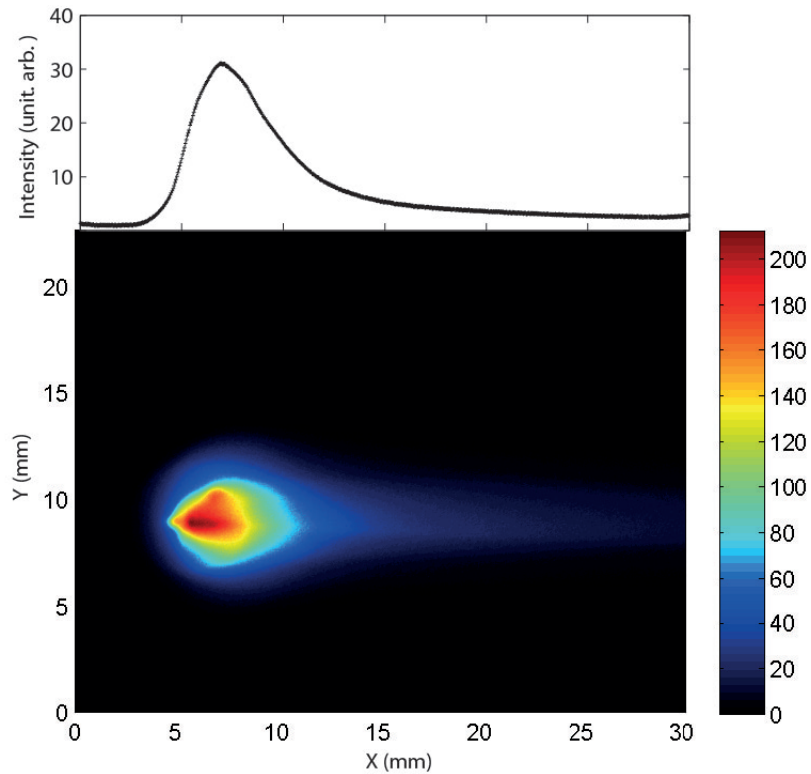


Figure 12. Visualisation of the transverse projection of the electron beam on the YAG:Ce screen located after the dipole in the dispersive region. The projected horizontal distribution is represented on the top of the image.

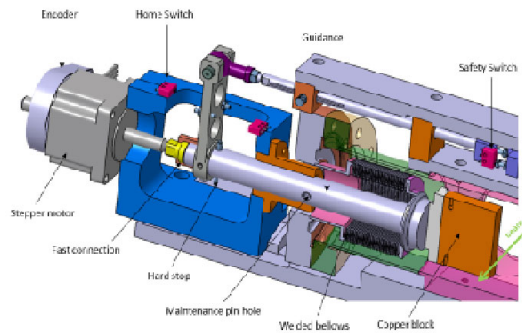


Figure 13. 3D view of the energy spread collimator. The copper block is actuated by a stepper and guided with the axle. The position is read by the encoder.

270 **4.3 Transverse dimensions**

271 The transverse sizes of the electron beam are measured with a YAG:Ce screen (YAG1) coupled to
 272 a CCD camera placed just before the coil in middle of the beam line (see fig. 1). The resolution
 273 of the optical system (made of one achromatic doublet) has been estimated to be about $80\mu\text{m}$.

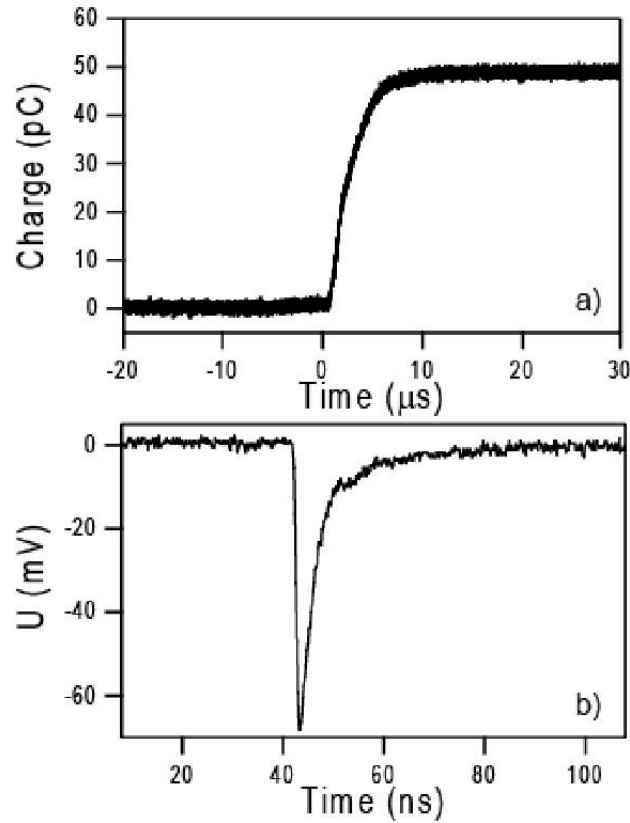


Figure 14. Signal of the a) ICT , b) Faraday cup.

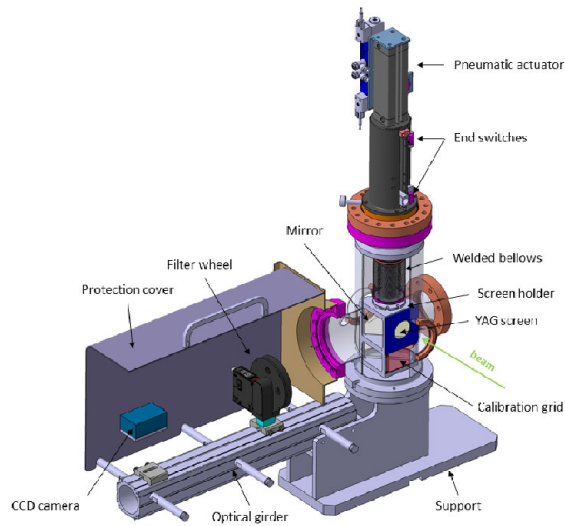


Figure 15. 3D view of the new screen station. The YAG:Ce screen at 90° from the beam is inserted on beam axis with the pneumatic actuator. The profile, reflected with a mirror at 45°, is analysed by a CCD camera at the end of the optical girder.

274 This resolution level is mainly induced by the orientation (45°) and the thickness (300 μm) of

275 the YAG:Ce screen [17]. A remote control filter wheel (equipped with discrete variable Optical
 276 Density) is placed just in front of the CCD in order to avoid image saturation. The cameras used
 277 are Blue Cougar Matrix Vision CCD camera type S123 (resp. S120) pixel size of 1360x1024 (resp.
 278 650x490).

279 A MATLAB code has been written in order to analyse the beam profile. A gaussian fit on
 280 the projected horizontal and vertical distributions enables to extract the diameter of the beam[18].
 281 An online extraction data HIM (based on Labview) is under development and will be operationnal
 282 in fews months [19]. Also a comparison of the fit gaussian method and the moment distribution
 283 method is in progress.

284 Three other YAG:Ce screens were installed in 2011 : one just before the dipole, a second at
 285 the end of the straight beam line and a third on the deviated beam line after the dipole. The optical
 286 system used for these stations are slightly different from the YAG1 station. The screen orientation
 287 is at 90° for YAG2, 3 and 4, instead of 45° for YAG1. A better resolution should be obtained
 288 with this set up. The light emitted by the YAG:Ce screen goes after a specular reflexion through
 289 an achromatic lenses doublet on the CCD pixel chip. The new YAG:Ce screen stations (see fig.
 290 15) are composed of a screen holder with a YAG:Ce screen perpendicular to the beam direction, a
 291 mirror placed at 45° and a calibration grid below, moved vertically with a two-position pneumatic
 292 jack, for checking the calibrartion pixels. We used only a simple guidance axis in order to have a
 293 basic, cheap and reliable system. The choice of avoiding the mechanical adjustments led us to have
 294 precise interfaces between the PHIL girder and the screen guidance but simplify the mounting and
 295 the operation of these screen stations (e.g. mirror or screen exchange).

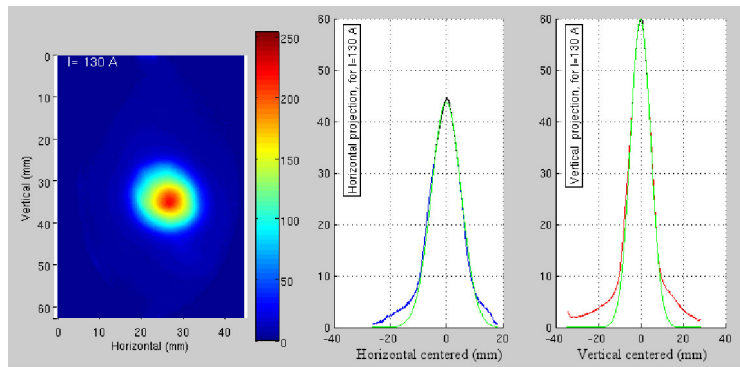


Figure 16. Left panel : transverse beam profile obtained on the YAG:Ce screen at 1925 mm from the photocathode, with a focusing solenoid (located at the exit of the Alphax gun) alimented by 130 A. Right panel : horizontal and vertical beam projection with gaussian fit (in green).

296 4.4 Bunch length

297 The bunch duration of the electron beam will be measured using a streak camera analysing the
 298 Cerenkov light emitted by the electrons crossing a thin saphir plate. The Cerenkov radiator is
 299 placed inside the beam pipe under vacuum. The Cerenkov light is transported over 15 m in air,
 300 inside a tubed path, up to the ARP streak camera, with metallic mirrors and achromatic lenses. We
 301 expect a rate of five photons per electron between 400 and 600 nm for a 5 MeV electron beam
 302 energy and $200\mu m$ saphir thickness. This is sufficient to have a good signal detected by the streak

303 camera. The resolution of our streak camera is 3ps. The complete set up of the bunch length is
304 under installation and will be available by 2013.

305 **4.5 Transverse emittance**

306 PHIL will be equipped with a two-dimensional transverse beam emittance measurement system
307 based on the multi-slits method. This technique - briefly described here - is realized by introducing
308 a slits mask in the beam trajectory, and by observing the output beamlets at a downstream location.
309 The position and the thickness of the beamlets allows to reconstruct the 2D trace space (x, x') or
310 (y, y') and the geometrical 2D rms transverse emittance [20]. The accuracy of the measurement
311 depends on the space charge effect, and all the parameters of the system should be carefully chosen
312 for a given range of beam setup [21]. For PHIL ($E < 10\text{MeV}$), a detailed analysis [22] has been
313 carried out using a home-made Matlab code [23]. This study fixed the following values for the
314 system [24]:

- 315 • mask material : tungsten (W)
- 316 • thickness of the mask : 3.5 mm
- 317 • number of slits : 27
- 318 • thickness of the slits : 0.1 mm
- 319 • distance between 2 slits : 1.5 mm
- 320 • distance between slits and screen : 230 mm

321 First measurement using this system are planned for 2013.

322 **5. Conclusion**

323 PHIL has commissioned several elements and can deliver electron beams routinely. Other elements
324 like the bunch length and emittance station measurement are expected to fully characterised the RF
325 guns. A full characterization of the beam, under different configurations will be done this year.
326 The understanding for sources of instabilities avoiding reproductibility is under characterisation in
327 order to be able to develop feedback systems. A first user experiment is expected during the year
328 2012.

329 **6. Acknowledgments**

330 We would like here to acknowledge the support of all people helping PHIL in a many ways starting
331 with the scientific committee of PHIL. The collaboration with CERN/CTF3 PHIN photoinjector
332 team also brings a lot to the PHIL developpement. Ideas given by the PITZ Zeuthen team are also
333 very helpful. We also thank the local radioprotection team without wich PHIL would not be able to
334 run. The support of the IN2P3 (Institut National de Physique Nucleaire et des Particules) and P2IO
335 (Physique des deux infinis) is also acknowledged here. The authors also acknowledge G. Bienvenu,
336 B. Mouton, B. Leblond, who initiated the design of PHIL during CARE.

337 **References**

- 338 [1] C. Travier, Etude, réalisation et expérimentation d'un canon hyperfréquence déclenché par un laser
339 subpicoseconde (candela), thèse université Paris-Sud.
- 340 [2] J. Rodier, T. Garvey, M. D. Loos, S. V. der Geer, S. Wiggins, V. Pavlov, Y. Saveliev, D. Jaroszynski,
341 Construction of the alpha-x photo-injector cavity, Proceedings of EPAC, <http://www.jacow.org> (2006)
342 1277–1279.
- 343 [3] J. Belloni, H. Monard, F. Gobert, J.-P. Larbre, A. Demarque, V. D. Waele, I. Lampre, J.-L. Marignier,
344 M. Mostafavi, J. Bourdon, M. Bernard, H. Borie, T. Garvey, B. Jacquemard, B. Leblond, P. Lepercq,
345 M. Omeïch, M. Roch, J. Rodier, R. Roux, Elyse, a picosecond electron accelerator for pulse radiolysis
346 research, Nuclear Instruments and Methods A 539 (2005) 527–539.
- 347 [4] R. Bossart, H. Braun, M. Dehler, J.-C. Godot, A 3 ghz photoelectron gun for high beam intensity,
348 Nuclear Instruments and Methods A 375 (1996) ABS7–ABS8.
- 349 [5] R. Roux, Conception of photo-injectors for the ctf3 experiment, Proceedings of the 46th workshop of
350 the INFN ELOISATRON project, The Physics and applications of high brightness electron beams
351 (2005) 237–253.
- 352 [6] J. Brossard, M. Desmons, B. Mercier, C. Prevost, R. Roux, Construction of the probe beam
353 photo-injector of ctf3, Proceedings of EPAC, <http://www.jacow.org> (2006) 828.
- 354 [7] R. Roux, S. Cavalier, M. Bernard, G. Bienvenu, M. Jore, B. Leblond, B. Mercier, B. Mouton,
355 C. Prevost, A. Variola, Phil: A test beamline at lal, proceeding of EPAC, <http://www.jacow.org> (2008)
356 2698–2700.
- 357 [8] R. Roux, C. Bruni, H. Monard, Design of a s-band 4.5 cells rf gun, Proceedings of
358 PAC, <http://www.jacow.org> (2011) 850.
- 359 [9] J. Rosado, F. Blanco, F. Arqueros, Comparison of available measurements of the absolute
360 fluorescence yield, arXiv 1004.3971v2.
- 361 [10] C. Bruni, N. Artemiev, R. Roux, A. Variola, F. Zomer, A. Loulergue, Thomx: A high flux compact x
362 ray source (2011) 49–55.
363 URL <http://dx.doi.org/10.1051/uvx/2011007>
- 364 [11] J. Brossard, F. Blot, S. Cavalier, A. Gonnin, M. Joré, P. Lepercq, S. Letourneur, B. Mercier,
365 H. Monard, C. Prevost, R. Roux, A. Variola, Phil accelerator at lal Ū diagnostics status, Proceedings
366 of BIW10, Santa Fe, US (2010) 446.
- 367 [12] H. Braun, R. Corsini, T. D'amico, J. Delahaye, G. Guignard, C. Johnson, A. Millich, P. Pearce,
368 L. Rinolfi, A. Riche, R. Ruth, D. Schulte, L. Thorndahl, M. Valentini, I. Wilson, W. Wuensch, The
369 clic rf power source, CERN yellow report CERN-99-06.
- 370 [13] M. Petrarca, H. Braun, E. Chevallay, S. Doebert, K. Elsener, V. Fedosseev, G. Geschonke, R. Losito,
371 A. Masi, O. Mete, L. Rinolfi, A. Dabrowski, M. Divall, N. Champault, G. Bienvenu, M. Jore,
372 B. Mercier, C. Prevost, R. Roux, C. Vicario, First results from commissioning of the phin
373 photo-injector for ctf3, Proceedings of PAC, <http://www.jacow.org> (2009) 509–511.
- 374 [14] J. Brossard, Annulation de l'induction magnétique sur la photocathode de la ligne phil : cas du canon
375 alphax, <http://phil.lal.in2p3.fr/spip.php?rubrique92> note PHIL n°2010-006.
- 376 [15] R. J. Brossard, S. Cavalier, Modélisation poisson du solénoïde de focalisation du photo-injecteur de
377 phil, <http://phil.lal.in2p3.fr/spip.php?rubrique92> note PHIL n°2010-005.

- 378 [16] M. Bernard, J. Bourdon, R. Chehab, T. Garvey, B. Jacquemard, B. Mouton, M. Omeich, J. Rodier,
379 P. Roudier, Y. Thiery, B. Aune, M. Desmons, J. Fusellier, J. Gournay, M. Jablonka, J. Joly,
380 M. Juillard, A. Mosnier, S. Buhler, T. Junquera, The tesla test facility linac injector, Proceedings of
381 EPAC, <http://www.jacow.org> (1994) 692–694.
- 382 [17] J. Brossard, Etude de systèmes optiques à un seul doublet achromatique pour l'imagerie transverse du
383 faisceau de phil, <http://phil.lal.in2p3.fr/spip.php?rubrique92> note PHIL n°2009-003.
- 384 [18] J. Brossard, Code matlab pour l'analyse des images, <http://phil.lal.in2p3.fr/spip.php?article110> note
385 PHIL n°2011-005.
- 386 [19] [link].
387 URL <http://phil.lal.in2p3.fr/spip.php?rubrique122>
- 388 [20] Min Zhang, Emittance formula for slits and pepper-pot measurement.
- 389 [21] S. G. Anderson, J. B. Rosenzweig, G. P. LeSage, J. K. Crane, Space-charge effects in high brightness
390 electron beam emittance measurements, Phys. Rev. ST Accel. Beams 5 (2002) 014201. .
391 URL <http://link.aps.org/doi/10.1103/PhysRevSTAB.5.014201>
- 392 [22] J. Brossard, Dimensionnement du mesureur d'émittance transverse de phil par la méthode des fentes,
393 <http://phil.lal.in2p3.fr/spip.php?rubrique92> note PHIL n°2011-011.
- 394 [23] J. Brossard, Matlab software used for the design of the 2d-transverse-emittance-meter system based
395 on the slits method, <http://phil.lal.in2p3.fr/spip.php?article145>.
- 396 [24] J. Brossard, Cahier des charges techniques du mesureur d'émittance transverse de phil par la méthode
397 des fentes, <http://phil.lal.in2p3.fr/spip.php?rubrique92> note PHIL n°2011-012.